Acta Crystallographica Section C
Crystal Structure Communications
ISSN 0108-2701

Nine closely related tetrahydro-1,4-epoxy-1-benzazepines carrying pendant heterocyclic substituents: hydrogen-bonded supramolecular assembly in zero, one and two dimensions

Maria C. Blanco,[a] Alirio Palma,[a] Justo Cobo[b] and Christopher Glidewell[c]*

[a]Laboratorio de Síntesis Orgánica, Escuela de Química, Universidad Industrial de Santander, AA 678 Bucaramanga, Colombia, [b]Departamento de Química Inorgánica y Orgánica, Universidad de Jaén, 23071 Jaén, Spain, and [c]School of Chemistry, University of St Andrews, Fife KY16 9ST, Scotland
Correspondence e-mail: cg@st-andrews.ac.uk

Received 7 February 2012
Accepted 16 February 2012
Online 24 February 2012

The structures are reported of nine closely related tetrahydro-1,4-epoxy-1-benzazepines carrying pendant heterocyclic substituents, namely: 2-*exo*-(5-nitrofuran-2-yl)-2,3,4,5-tetrahydro-1,4-epoxy-1*H*-1-benzazepine, $C_{14}H_{12}N_2O_4$, (I), 7-fluoro-2-*exo*-(1-methyl-1*H*-pyrrol-2-yl)-2,3,4,5-tetrahydro-1,4-epoxy-1*H*-1-benzazepine, $C_{15}H_{15}FN_2O$, (II), 7-fluoro-2-*exo*-(5-methylfuran-2-yl)-2,3,4,5-tetrahydro-1,4-epoxy-1*H*-1-benzazepine, $C_{15}H_{14}FNO_2$, (III), 7-fluoro-2-*exo*-(3-methylthiophen-2-yl)-2,3,4,5-tetrahydro-1,4-epoxy-1*H*-1-benzazepine, $C_{15}H_{14}FNOS$, (IV), 7-fluoro-2-*exo*-(5-methylthiophen-2-yl)-2,3,4,5-tetrahydro-1,4-epoxy-1*H*-1-benzazepine, $C_{15}H_{14}FNOS$, (V), 7-chloro-2-*exo*-(5-methylfuran-2-yl)-2,3,4,5-tetrahydro-1,4-epoxy-1*H*-1-benzazepine, $C_{15}H_{14}ClNO_2$, (VI), 2-*exo*-(5-methylfuran-2-yl)-7-trifluoromethoxy-2,3,4,5-tetrahydro-1,4-epoxy-1*H*-1-benzazepine, $C_{16}H_{14}F_3NO_3$, (VII), 2-*exo*-(3-methylthiophen-2-yl)-7-trifluoromethoxy-2,3,4,5-tetrahydro-1,4-epoxy-1*H*-1-benzazepine, $C_{16}H_{14}F_3NO_2S$, (VIII), and 2-*exo*-(5-nitrofuran-2-yl)-7-trifluoromethoxy-2,3,4,5-tetrahydro-1,4-epoxy-1*H*-1-benzazepine, $C_{15}H_{11}F_3N_2O_5$, (IX). All nine compounds crystallize in centrosymmetric space groups as racemic mixtures with configuration (2*RS*,4*SR*). There are no direction-specific interactions between the molecules in (V). The molecules in (III), (IV), (VI) and (VII) are linked into simple chains, by means of a single C—H$\cdots$O hydrogen bond in each of (III), (VI) and (VII), and by means of a single C—H$\cdots\pi$(arene) hydrogen bond in (IV), while the molecules in (VIII) are linked into a chain of rings. In each of (I) and (II), a combination of one C—H$\cdots$O hydrogen bond and one C—H$\cdots\pi$(arene) hydrogen bond links the molecules into sheets, albeit of completely different construction in the two compounds. In (IX), the sheet structure is built from a combination of four independent C—H$\cdots$O hydrogen bonds and one C—H$\cdots\pi$(arene) hydrogen bond. Comparisons are made with some related compounds.

Comment

We report here the molecular and supramolecular structures of nine closely related tetrahydro-1,4-epoxy-1-benzazepines carrying pendant heterocyclic substituents, compounds (I)–(IX) (Fig. 1 and Scheme 1), and we compare these with some related compounds whose structures were reported recently, *viz.* (X)–(XII) (Blanco *et al.*, 2008) and (XIII)–(XV) (Blanco *et al.*, 2009) (Scheme 2). The work reported here continues our structural study of this class of epoxybenzazepines (Acosta *et al.*, 2008; Blanco *et al.*, 2008, 2009; Gómez *et al.*, 2008, 2009), which is itself associated with a synthetic programme to identify structurally novel antiparasitic agents having new modes of action against both *Trypanosoma cruzi* and *Leishmania chagasi* (Gómez *et al.*, 2008; Yépez *et al.*, 2006; Gómez-Ayala *et al.*, 2010). Compounds (I)–(IX) were all prepared by appropriate modification of the procedure reported previously by Acosta *et al.* (2008).

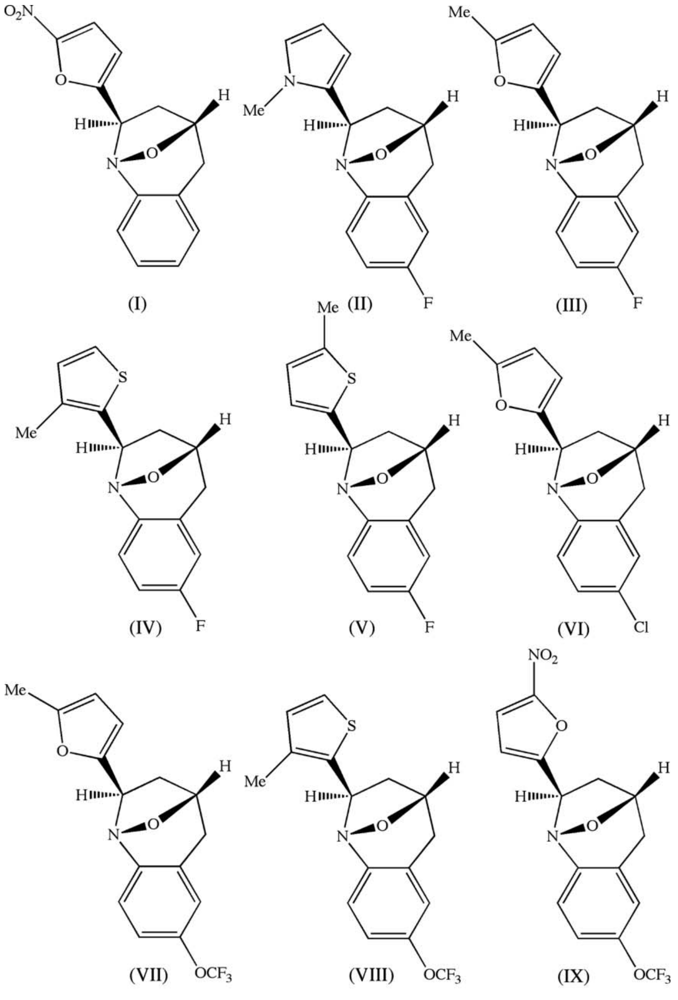

Scheme 1

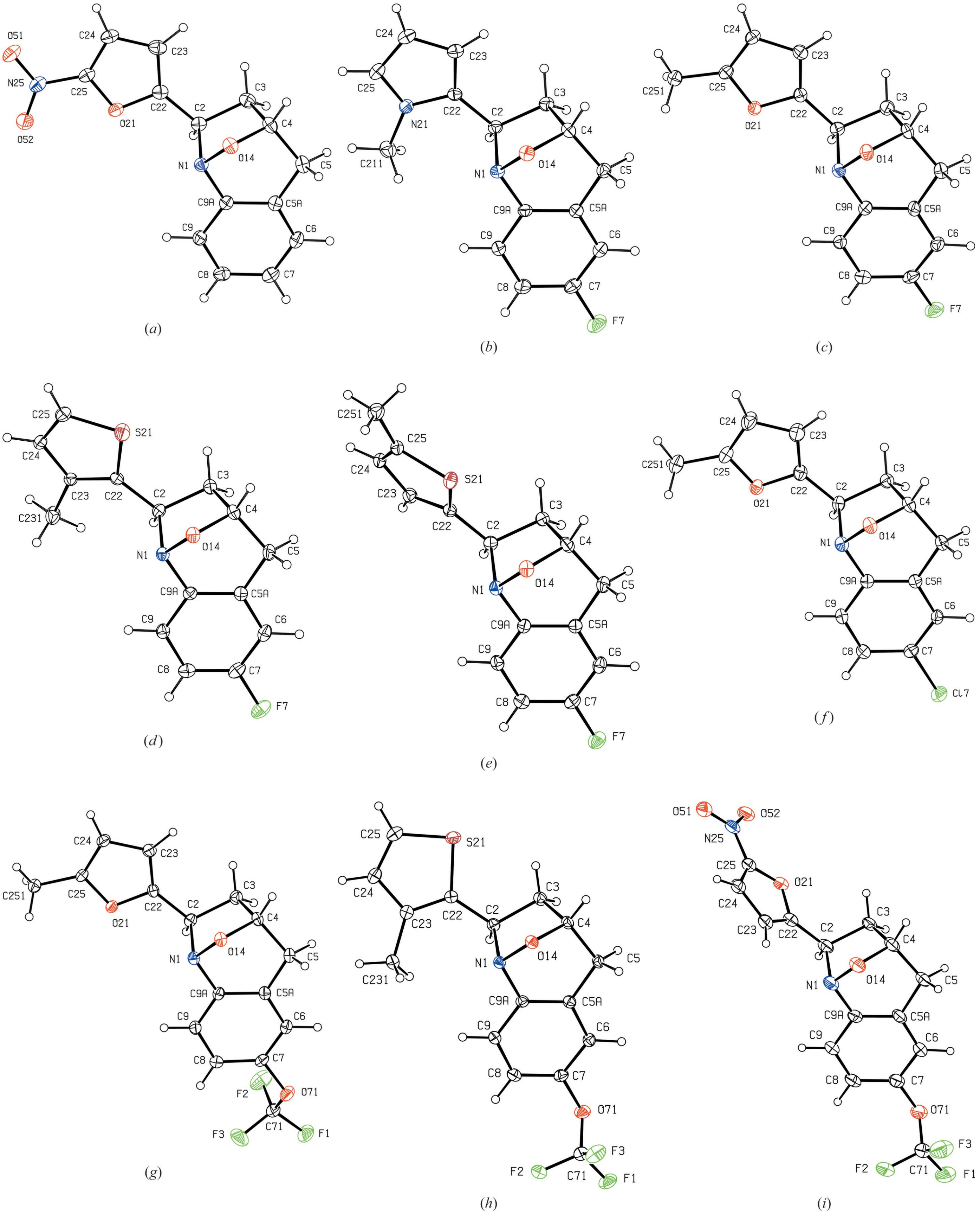

Figure 1

The molecular structures of (I)–(IX), showing the atom-labelling schemes for (*a*) compound (I), (*b*) (II), (*c*) (III), (*d*) (IV), (*e*) (V), (*f*) (VI), (*g*) (VII), (*h*) (VIII) and (*i*) (IX). Displacement ellipsoids are drawn at the 30% probability level.

The molecular constitutions of (I)–(XV) differ in just two respects: (i) the identity of the simple substituent at position 7 (*cf*. Fig. 1) and (ii) the nature of the heterocyclic substituent at position 2. Of the compounds newly reported here, (II)–(V), along with the previously reported (X) and (XI) (Blanco *et al.*, 2008), all carry a fluoro substituent at position 7, and (VI), along with (XIII) and (XV) (Blanco *et al.*, 2009), has a chloro substituent at this position, while (VII)–(IX), and (XII) (Blanco *et al.*, 2008), all have a trifluoromethoxy substituent at position 7. The substituents at position 2 comprise a variety of simply substituted furan units in (I), (III), (VI), (VII), (IX) and (X), or thienyl units in (IV), (V), (VIII) and (XI)–(XV), with a substituted pyrrole unit in (II). Compounds (I)–(IX) all crystallize in centrosymmetric space groups, with $Z' = 1$. The molecules contain two stereogenic centres, at atoms C2 and C4, and the reference molecules in (I)–(IX) were all selected to have the *R* configuration at atom C2 and, on this basis, the configuration at atom C4 is always *S* in the reference molecules. The space groups for (I)–(IX) indicate that these compounds all crystallize as true racemates with configurations (2*RS*,4*SR*). By contrast, (X) crystallizes with $Z' = 2$ in the centrosymmetric space group $P2_1/c$, while (XII) crystallizes in the Sohnke space group $P2_1$ with $Z' = 1$ as a single enantiomorph, having configuration (2*S*,4*R*) in the crystal selected for data collection (Blanco *et al.*, 2008).

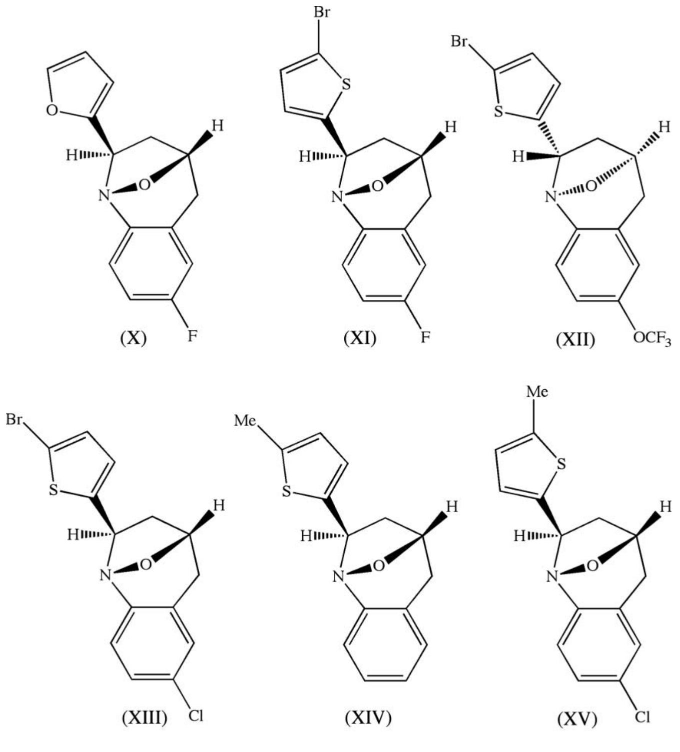

Scheme 2

The shapes of the heterobicyclic ring systems in (I)–(VII) and (IX) are all very similar, as indicated by the ring-puckering parameters (Cremer & Pople, 1975), while (VIII) differs somewhat (Table 1). In each of (I)–(VII) and (IX), the five-membered ring adopts a half-chair conformation, for which the idealized value of the puckering angle φ is $(36k + 18)^\circ$, where k represents an integer. On the other hand, this ring in (VIII) adopts a conformation close to an envelope form, folded across the line N1$\cdots$C4, where the ideal value of φ is $(36k)^\circ$. The six-membered rings all adopt conformations intermediate between a half-chair form, where the idealized values of the puckering angles are $\theta = 129.2^\circ$ and $\varphi = (60k + 30)^\circ$, and an envelope form, where the idealized values are $\theta =$

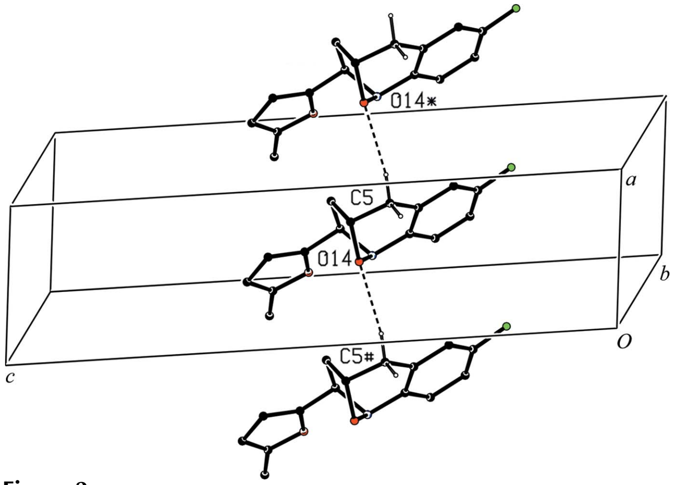

Figure 2
Part of the crystal structure of (III), showing the formation of a hydrogen-bonded *C*(4) chain running parallel to [100]. For the sake of clarity, H atoms bonded to C atoms not involved in the motif shown have been omitted. Atoms marked with an asterisk (*) or a hash symbol (#) are at the symmetry positions ($x + 1$, y, z) and ($x - 1$, y, z), respectively.

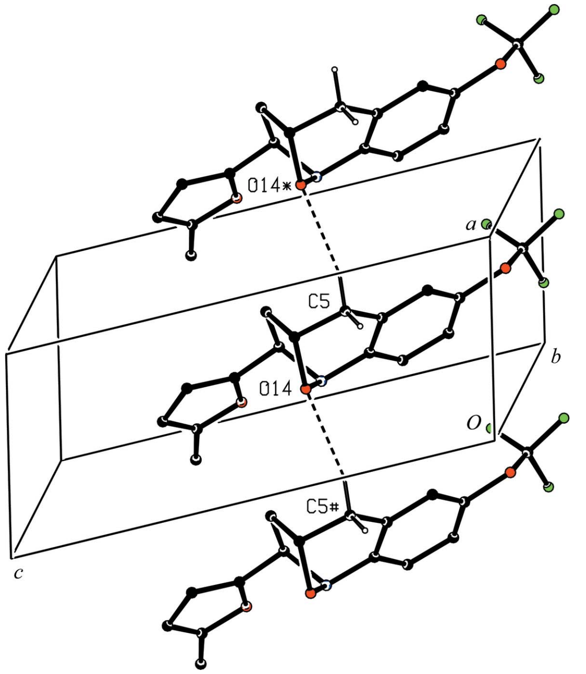

Figure 3
Part of the crystal structure of (VII), showing the formation of a hydrogen-bonded *C*(4) chain running parallel to [100]. For the sake of clarity, H atoms bonded to C atoms not involved in the motif shown have been omitted. Atoms marked with an asterisk (*) or a hash symbol (#) are at the symmetry positions ($x + 1$, y, z) and ($x - 1$, y, z), respectively.

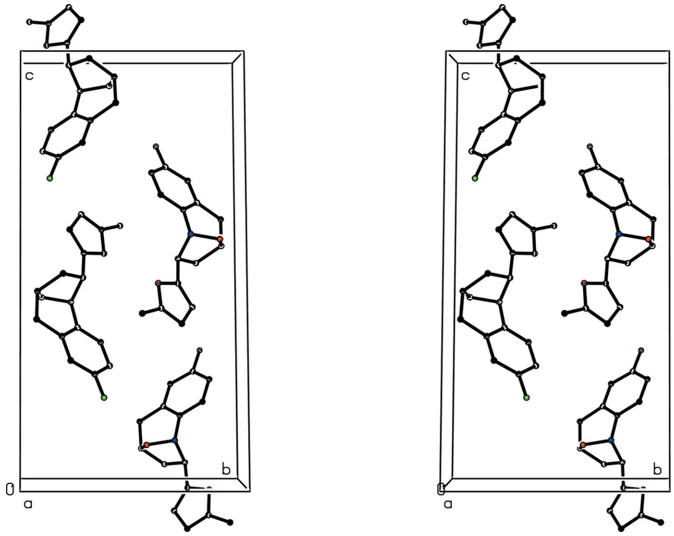

Figure 4
A stereoview of part of the crystal structure of (III), viewed approximately along [100], showing the arrangement of the four chains passing through each unit cell. For the sake of clarity, H atoms have been omitted.

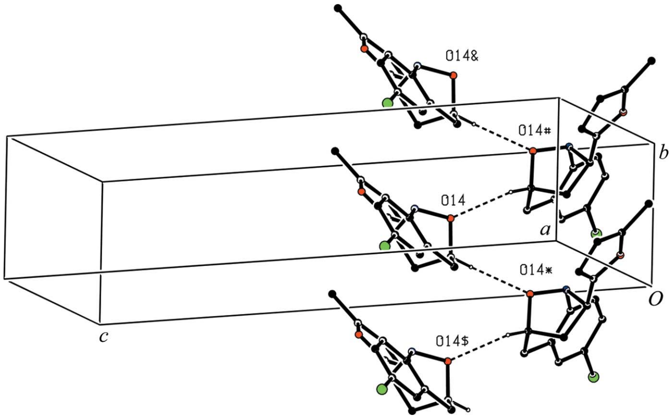

Figure 5
Part of the crystal structure of (VI), showing the formation of a hydrogen-bonded $C(3)$ chain running parallel to [010]. For the sake of clarity, H atoms bonded to C atoms not involved in the motif shown have been omitted. Atoms marked with an asterisk (*), a hash symbol (#), a dollar sign ($) or an ampersand (&) are at the symmetry positions $(-x + \frac{1}{2}, y - \frac{1}{2}, -z + \frac{1}{2})$, $(-x + \frac{1}{2}, y + \frac{1}{2}, -z + \frac{1}{2})$, $(x, y - 1, z)$ and $(x, y + 1, z)$, respectively.

125.3° and $\varphi = (60k)°$, where k represents an integer in each case.

The supramolecular assemblies in (I)–(IX) are dominated by C—H···O and C—H···π(arene) hydrogen bonds, although a C—H···π(thienyl) interaction is present in the structure of (VIII) (Table 2). The criteria for the acceptance of such intermolecular interactions as structurally significant may be simply stated: (i) C—H···O contacts have been discounted if the C—H···O angle is significantly less than 140° (*cf.* Wood *et al.*, 2009); (ii) C—H···π contacts have been discounted if the H···(ring centroid) distance exceeds 2.90 Å; (iii) all contacts involving methyl C—H bonds have been discounted; and (iv) C—H···F contacts have all been discounted (Howard *et al.*, 1996; Brammer *et al.*, 2001; Thallypally & Nangia, 2001). In addition, we may note here that none of the structures of (I)–(IX) exhibits any aromatic π–π stacking interactions.

Subject to the criteria enumerated above, it is convenient to discuss the supramolecular assembly of (I)–(IX) in order of increasing complexity, and then briefly to compare these supramolecular structures with those of the related compounds, (X)–(XV) (Blanco *et al.*, 2008).

There are no direction-specific intermolecular interactions of any kind in the structure of (V), so that this structure may be regarded as zero-dimensional, built from essentially isolated molecules. In each of (III) and (VII), which carry the same heterocyclic substituent but different substituents at position 7 (see Scheme 1), a single rather long but almost linear C—H···O hydrogen bond links molecules related by translation into $C(4)$ (Bernstein *et al.*, 1995) chains running parallel to the [100] direction (Figs. 2 and 3). Two such chains, related to one another by inversion, pass through each unit cell in (VII), but there are four chains passing through each unit cell in (III) (Fig. 4).

In the structure of (VI), the molecules are again linked into a chain by a single C—H···O hydrogen bond (Table 2), but now the chain is of $C(3)$ type running parallel to the [010] direction, and the component molecules are related by a 2_1 screw axis (Fig. 5). The chains in (IV) are built from a single C—H···π(arene) hydrogen bond linking molecules related by an n-glide plane, such that the chain is parallel to the $[10\overline{1}]$ direction (Fig. 6). In the structure of (VIII), molecules related by translation along [010] are linked into $C(4)$ chains by a C—H···O hydrogen bond (Fig. 7), exactly analogous to the chain formation in (III) and (VII). However, the action of the C—H···O hydrogen bond in (VIII) is modestly augmented by a C—H···π(thienyl) contact, so that the hydrogen-bonded assembly here should more properly be regarded as a chain of rings. Thus, for each of (III), (IV), (VI), (VII) and (VIII), the supramolecular assembly takes the form of a one-dimensional

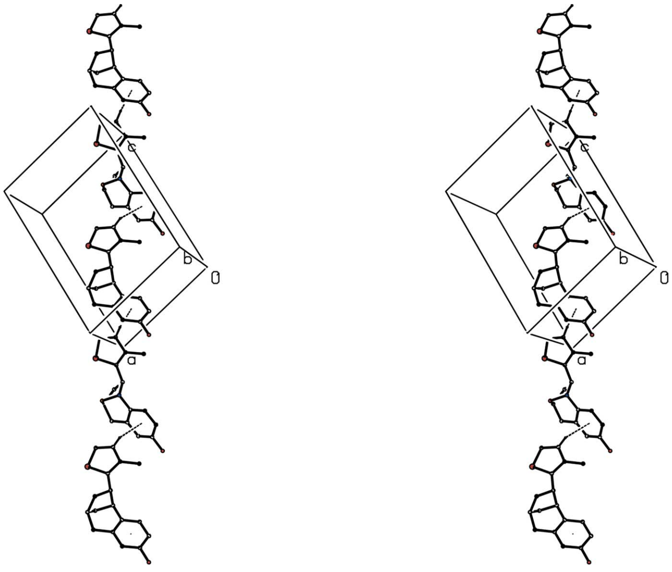

Figure 6
A stereoview of part of the crystal structure of (IV), showing the formation of a hydrogen-bonded chain running parallel to $[10\overline{1}]$. For the sake of clarity, H atoms bonded to C atoms not involved in the motif shown have been omitted.

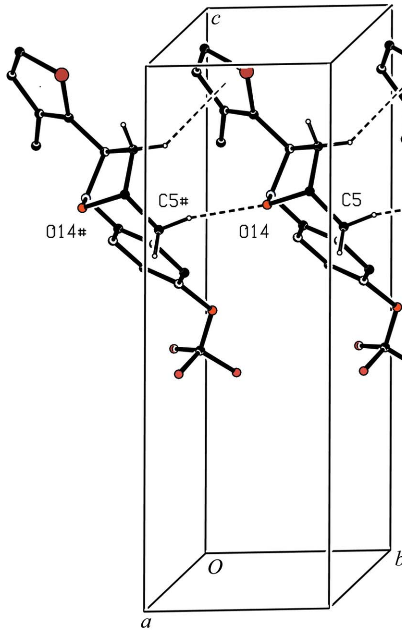

Figure 7
Part of the crystal structure of (VIII), showing the formation of a hydrogen-bonded *C*(4) chain running parallel to [010]. For the sake of clarity, H atoms bonded to C atoms not involved in the motif shown have been omitted. Atoms marked with an asterisk (*) or a hash symbol (#) are at the symmetry positions (x, $y + 1$, z) and (x, $y - 1$, z), respectively.

hydrogen-bonded structure, with simple chains in the first four of these compounds and a chain of rings in (VIII).

The hydrogen-bonded supramolecular assembly in each of (I) and (II) is two-dimensional and, in each case, the sheet structure is built from a combination of one C—H⋯O hydrogen bond and one C—H⋯π(arene) hydrogen bond. However, except for the π(arene) acceptor, the donors and acceptors all differ (Table 2), so that the construction of the sheet is also different in the two compounds.

The formation of the sheet structure in (II) is readily analysed in terms of two one-dimensional substructures, each in the form of a simple chain involving just one type of hydrogen bond. Molecules of (II) related by translation are linked by a C—H⋯O hydrogen bond to form a *C*(4) chain running parallel to the [010] direction, analogous to the *C*(4) chains in (III) and (VII). In addition, molecules of (II) related by a *c*-glide plane are linked by a C—H⋯π(arene) hydrogen bond into a chain running parallel to the [001] direction. The combination of these two simple chain motifs generates a sheet lying parallel to (100) and containing just one type of ring (Fig. 8).

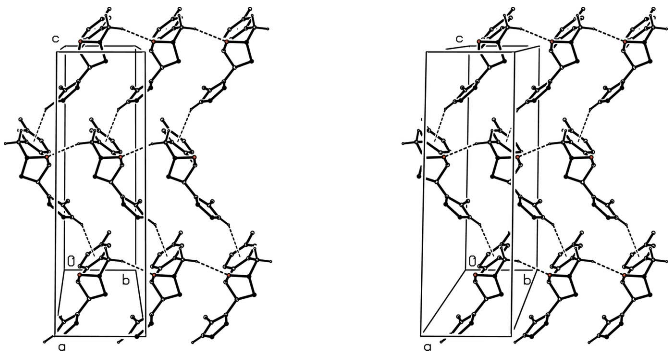

Figure 8
A stereoview of part of the crystal structure of (II), showing the formation of a hydrogen-bonded sheet parallel to (100) and containing only a single type of ring. For the sake of clarity, H atoms bonded to C atoms not involved in the motifs shown have been omitted.

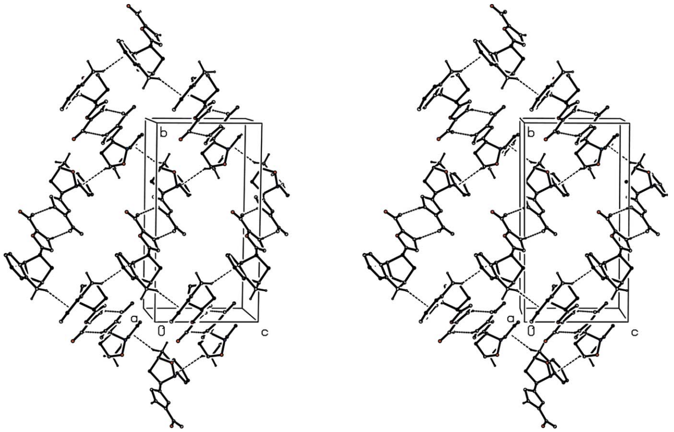

Figure 9
A stereoview of part of the crystal structure of (I), showing the formation of a hydrogen-bonded sheet parallel to (100) and containing two types of ring. For the sake of clarity, H atoms bonded to C atoms not involved in the motifs shown have been omitted.

In the structure of (I), by contrast, a C—H⋯O hydrogen bond links pairs of molecules which are related by inversion to form a cyclic centrosymmetric dimeric unit characterized by an $R_2^2(10)$ motif. This dimeric unit is centred across $(0, \frac{1}{2}, 0)$ and it may conveniently be regarded as the basic building block in the formation of the sheet structure of (I). The dimer centred across $(0, \frac{1}{2}, 0)$ is directly linked by a C—H⋯π(arene) hydrogen bond to four further such dimers, centred respectively across $(0, 0, \frac{1}{2})$, $(0, 0, -\frac{1}{2})$, $(0, 1, \frac{1}{2})$ and $(0, 1, -\frac{1}{2})$, so

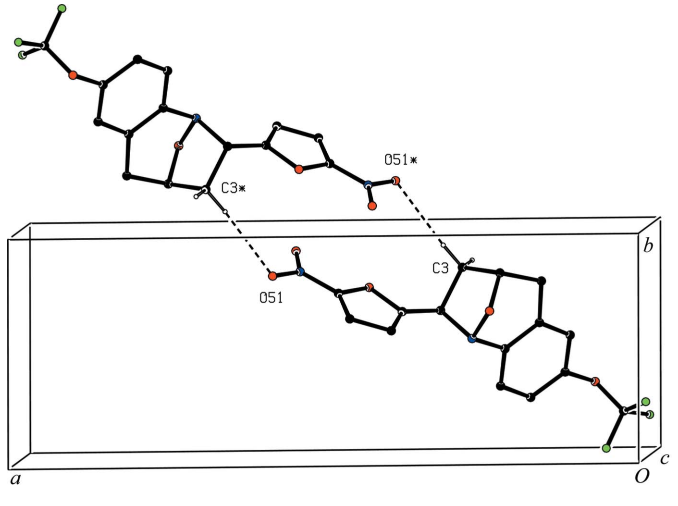

Figure 10
Part of the crystal structure of (IX), showing the formation of a cyclic centrosymmetric $R_2^2(16)$ motif. For the sake of clarity, H atoms bonded to C atoms not involved in the motif shown have been omitted. Atoms marked with an asterisk (*) are at the symmetry position ($-x + 1$, $-y + 2$, $-z + 1$).

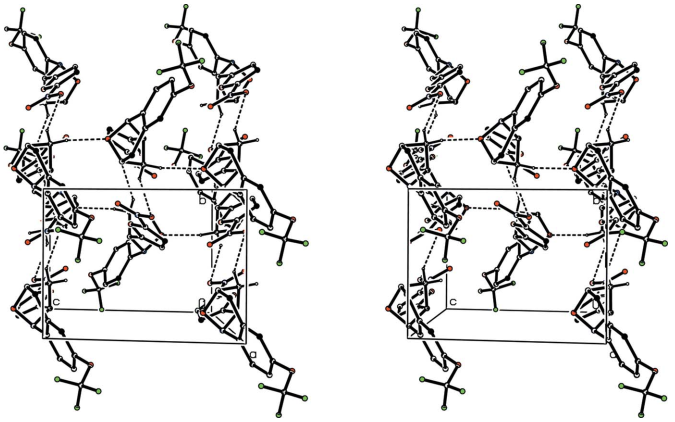

Figure 11
A stereoview of part of the crystal structure of (IX), showing the action of the hydrogen bond involving atom H3*B* in the linking of the $R_2^2(16)$ dimers. For the sake of clarity, H atoms bonded to C atoms not involved in the motifs shown have been omitted.

forming a sheet lying parallel to (100) and containing two types of ring, both of them centrosymmetric (Fig. 9).

The sheet structure of (IX) is considerably more complex than those in (I) and (II) as five independent hydrogen bonds are involved, four of C—H$\cdots$O type and one of C—H$\cdots\pi$(arene) type (Table 2). However, the essential features of the sheet formation can be conveniently, although not uniquely, analysed in terms of just three of the C—H$\cdots$O hydrogen bonds. Just as for (I), so too for (IX), a cyclic centrosymmetric dimer unit can be regarded as the basic building block for the sheet structure, but in the structure of (IX) the dimer motif is of $R_2^2(16)$ type (Fig. 10), as opposed to the $R_2^2(10)$ motif in (I). This reference dimer is centred across $(\frac{1}{2}, 1, \frac{1}{2})$ and the C—H$\cdots$O hydrogen bond which involves atom H3*B* (Table 2) links this dimer directly to the four similar dimer units centred across $(\frac{1}{2}, \frac{1}{2}, 1)$, $(\frac{1}{2}, \frac{1}{2}, 0)$, $(\frac{1}{2}, \frac{3}{2}, 1)$ and $(\frac{1}{2}, \frac{3}{2}, 0)$ (Fig. 11). In addition, the same reference dimer across $(\frac{1}{2}, 1, \frac{1}{2})$ is linked by the C—H$\cdots$O hydrogen bond involving atom H8 to four further dimeric units, centred across $(\frac{1}{2}, -\frac{1}{2}, 1)$, $(\frac{1}{2}, -\frac{1}{2}, 0)$, $(\frac{1}{2}, \frac{5}{2}, 1)$ and $(\frac{1}{2}, \frac{5}{2}, 0)$ (Fig. 12). These interactions in combination give rise to a complex sheet lying parallel to (100). The remaining two hydrogen bonds both lie within the sheet, so that they serve to augment its strength and increase its complexity, but they do not influence the overall dimensionality of the hydrogen-bonded assembly.

We briefly compare here the structures of (X)–(XV) (Blanco *et al.*, 2008, 2009) with those of (I)–(IX). In the structure of (X), which crystallizes with $Z' = 2$, a combination of one C—H$\cdots$N hydrogen bond and three C—H$\cdots$O hydrogen bonds links the molecules into a chain of edge-fused $R_4^3(20)$ rings, antiparallel pairs of which are weakly linked by two rather long C—H$\cdots\pi$(arene) hydrogen bonds. It is noteworthy that (X) is the only example amongst (I)–(XII) where the Z' value is other than 1 and the only example where the structure contains a C—H$\cdots$N hydrogen bond.

As with the closely related (V), there are no hydrogen bonds of any kind in the structure of (XI), although the molecules of (XI) are weakly linked into centrosymmetric dimers by a single aromatic π–π stacking interaction involving the fluoro-substituted ring. Compounds (V) and (XI) both crystallize in the space group $P2_1/c$ with $Z' = 1$, and with somewhat similar unit-cell dimensions. Comparison of the two sets of atomic coordinates shows that these also are somewhat similar, but with sufficient differences in detail that (V) and (XI) could, at best, be described as only approximately isostructural. In particular, the π–π stacking interaction present in the structure of (XI) is absent from the structure of (V).

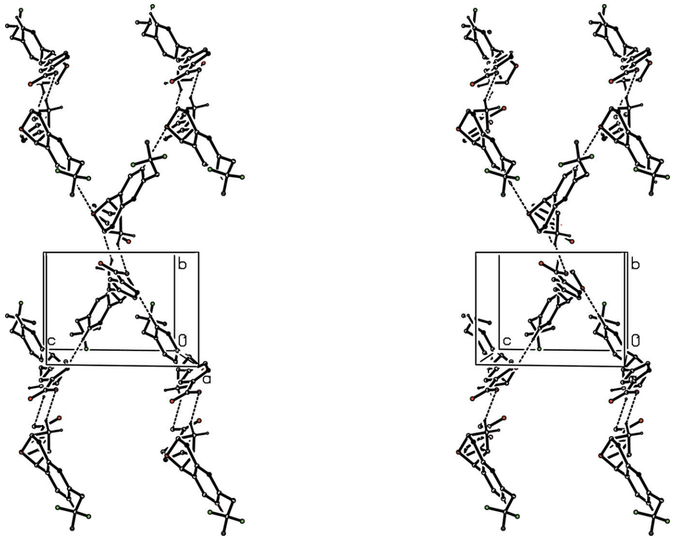

Figure 12
A stereoview of part of the crystal structure of (IX), showing the action of the hydrogen bond involving atom H8 in the linking of the $R_2^2(16)$ dimers. For the sake of clarity, H atoms bonded to C atoms not involved in the motifs shown have been omitted.

Compound (XII) is the only example in the series (I)–(XV) which crystallizes as a single enantiomorph. The molecules of (XII) are linked by two C—H$\cdots$O hydrogen bonds, both having the fused-ring O atom as the acceptor, to form a sheet containing a single type of $R_4^3(20)$ ring.

Although (XIII) and (XIV) both crystallize with $Z' = 1$ in the space group *Pbca*, the unit-cell dimensions for these two compounds are very different, as are their modes of supramolecular assembly. Paired C—H$\cdots\pi$(thienyl) hydrogen bonds link molecules of (XIII) into centrosymmetric dimers, while a combination of C—H$\cdots$O and C—H$\cdots\pi$(thienyl) hydrogen bonds links the molecules of (XIV) into a chain of rings. A more complex chain of rings is formed in (XV) built from four independent hydrogen bonds, two of C—H$\cdots$O type and one each of C—H$\cdots\pi$(thienyl) and C—H$\cdots\pi$(arene) types.

Accordingly, despite the rather small differences in molecular composition and molecular constitution amongst the members of the series (I)–(XV), no two of the compounds display the same pattern of supramolecular assembly.

Experimental

For the synthesis of (I)–(IX), sodium tungstate dihydrate (10% mol), followed by 30% aqueous hydrogen peroxide solution (12 mmol),

Table 1
Ring-puckering parameters (Å, °) for (I)–(IX).

Ring-puckering angles in the five-membered rings refer to the atom sequence O14—N1—C2—C3—C4, those in the six-membered rings to O14—N1—C9a—C5a—C5—C4 and those in the seven-membered rings to N1—C2—C3—C4—C5—C5a—C9a.

(*a*)	Five-membered rings	
Compound	Q_2	φ_2
(I)	0.444 (2)	13.3 (3)
(II)	0.445 (2)	16.9 (3)
(III)	0.444 (2)	19.5 (3)
(IV)	0.447 (2)	16.2 (3)
(V)	0.457 (2)	18.8 (3)
(VI)	0.446 (2)	15.4 (3)
(VII)	0.443 (3)	14.7 (4)
(VIII)	0.434 (2)	4.5 (3)
(IX)	0.448 (2)	17.0 (3)

(*b*)	Six-membered rings		
Compound	Q	θ	φ
(I)	0.607 (2)	130.0 (2)	164.7 (2)
(II)	0.616 (2)	129.7 (2)	166.3 (3)
(III)	0.617 (2)	130.5 (2)	162.3 (3)
(IV)	0.621 (2)	128.2 (2)	166.3 (3)
(V)	0.625 (2)	127.0 (2)	163.9 (2)
(VI)	0.609 (2)	130.6 (2)	165.0 (3)
(VII)	0.613 (2)	129.6 (2)	165.2 (3)
(VIII)	0.606 (2)	128.8 (2)	170.1 (3)
(IX)	0.627 (4)	126.8 (4)	162.5 (5)

(*c*)	Seven-membered rings		
Compound	Q	φ_2	φ_3
(I)	1.126 (2)	16.62 (11)	300.6 (4)
(II)	1.123 (2)	16.61 (12)	297.8 (4)
(III)	1.143 (2)	14.76 (12)	297.8 (4)
(IV)	1.111 (2)	16.39 (13)	298.8 (4)
(V)	1.108 (2)	14.36 (13)	297.6 (4)
(VI)	1.132 (2)	16.55 (12)	298.8 (4)
(VII)	1.125 (2)	16.77 (15)	300.2 (5)
(VIII)	1.109 (2)	21.02 (13)	306.8 (4)
(IX)	1.117 (4)	14.4 (2)	299.0 (7)

Table 2
Hydrogen-bond parameters (Å, °) for (I)–(IV) and (VI)–(IX).

*Cg*1 represents the centroid of the C5a/C6–C9/C9a ring and *Cg*2 represents the centroid of the S21/C22–C25 ring.

D—H···*A*	*D*—H	H···*A*	*D*···*A*	*D*—H···*A*
(I)				
C24—H24···O51^{i}	0.95	2.45	3.359 (3)	161
C5—H5*B*···*Cg*1^{ii}	0.99	2.66	3.458 (2)	138
(II)				
C5—H5*A*···O14^{iii}	0.99	2.58	3.530 (3)	161
C25—H25···*Cg*1^{iv}	0.95	2.81	3.654 (2)	149
(III)				
C5—H5*A*···O14^{v}	0.99	2.55	3.527 (3)	169
(IV)				
C24—H24···*Cg*1^{vi}	0.95	2.56	3.443 (3)	154
(VI)				
C4—H4···O14^{vii}	1.00	2.49	3.312 (3)	140
(VII)				
C5—H5*A*···O14^{v}	0.99	2.58	3.545 (3)	165
(VIII)				
C5—H5*A*···O14^{viii}	0.99	2.41	3.383 (3)	168
C3—H3*A*···*Cg*2^{viii}	0.99	2.70	3.533 (3)	142
(IX)				
C3—H3*A*···O51^{ix}	0.99	2.59	3.502 (5)	153
C3—H3*B*···O14^{x}	0.99	2.50	3.475 (5)	170
C8—H8···O14^{xi}	0.95	2.48	3.412 (6)	165
C24—H24···O52^{ii}	0.95	2.42	3.340 (6)	162
C4—H4···*Cg*1^{ii}	1.00	2.84	3.751 (5)	152

Symmetry codes: (i) $-x, -y+1, -z$; (ii) $x, -y+\frac{3}{2}, z-\frac{1}{2}$; (iii) $x, y-1, z$; (iv) $x, -y+2, z-\frac{1}{2}$; (v) $x+1, y, z$; (vi) $x-\frac{1}{2}, -y+\frac{1}{2}, z+\frac{1}{2}$; (vii) $-x+\frac{1}{2}, y-\frac{1}{2}, -z+\frac{1}{2}$; (viii) $x, y+1, z$; (ix) $-x+1, -y+2, -z+1$; (x) $x, -y+\frac{3}{2}, z+\frac{1}{2}$; (xi) $x, -y+\frac{1}{2}, z+\frac{1}{2}$.

were added to a stirred and cooled (ice bath) solution of the appropriately substituted 2-allyl-*N*-(heteroarylmethyl)aniline (4 mmol) in methanol (30 ml). The resulting mixtures were stirred at 273 K for 2–8 h and then at ambient temperature for an additional 12–20 h. Each mixture was filtered and then extracted with ethyl acetate (2 × 50 ml) and, for each, the combined extracts were dried over anhydrous sodium sulfate. The solvent was removed under reduced pressure and toluene (30 ml) was added to the resulting solid residue. These mixtures were heated under reflux for 6–8 h and, after cooling each solution to ambient temperature, the solvent was removed under reduced pressure and the crude product was subjected to column chromatographic resolution over silica gel using heptane–ethyl acetate (compositions ranged from 50:1 to 10:1 *v*/*v*) as eluent. Crystallization from heptane or heptane–ethyl acetate gave crystals suitable for single-crystal X-ray diffraction. Compound (I), pale yellow, yield 64%, m.p. 411 K; MS (70 eV) *m*/*z* (%): 272 (M^+, 30), 255 (3), 242 (3), 130 (10), 104 (100), 105 (67). Compound (II), colourless, yield 21%, m.p. 427 K; MS (70 eV) *m*/*z* (%): 258 (M^+, 30), 241 (18), 228 (1), 148 (9), 123 (9), 122 (15), 107 (100). Compound (III), colourless, yield 60%, m.p. 375 K; MS (70 eV) *m*/*z* (%): 259 (M^+, 33), 242 (18), 229 (6), 148 (9), 123 (27), 122 (52), 108 (100). Compound (IV), colourless, yield 66%, m.p. 399 K; MS (70 eV) *m*/*z* (%): 275 (M^+, 52), 258 (30), 245 (9), 148 (15), 124 (79), 123 (91), 122 (100). Compound (V), colourless, yield 64%, m.p. 376 K; MS (70 eV) *m*/*z* (%): 275 (M^+, 52), 258 (36), 245 (12), 148 (12), 124 (100), 123 (82), 122 (79). Compound (VI), colourless, yield 67%, m.p. 386 K; MS (70 eV) *m*/*z* (%): 275 (M^+, ^{35}Cl, 18), 258 (12), 245 (3), 164 (6), 139 (27), 138 (33), 108 (100). Compound (VII), colourless, yield 57%, m.p. 366 K; MS (70 eV) *m*/*z* (%): 325 (M^+, 18), 308 (12), 295 (3), 214 (6), 189 (27), 188 (45), 108 (100). Compound (VIII), colourless, yield 69%, m.p. 351 K; MS (70 eV) *m*/*z* (%): 341 (M^+, 30), 324 (21), 311 (6), 214 (9), 189 (67), 188 (100), 124 (70). Compound (IX), pale yellow, yield 56%, m.p. 438 K; MS (70 eV) *m*/*z* (%): 356 (M^+, 9), 339 (1), 326 (1), 214 (12), 189 (70), 188 (100).

Compound (I)

Crystal data

$C_{14}H_{12}N_2O_4$
$M_r = 272.26$
Monoclinic, $P2_1/c$
$a = 7.2248\ (5)$ Å
$b = 18.1447\ (19)$ Å
$c = 9.4504\ (8)$ Å
$\beta = 94.279\ (6)°$
$V = 1235.42\ (19)$ Å^3
$Z = 4$
Mo *K*α radiation
$\mu = 0.11$ mm^{-1}
$T = 120$ K
0.38 × 0.27 × 0.22 mm

Data collection

Bruker–Nonius KappaCCD area-detector diffractometer
Absorption correction: multi-scan (*SADABS*; Sheldrick, 2003)
$T_{min} = 0.960$, $T_{max} = 0.976$
18226 measured reflections
2835 independent reflections
1868 reflections with $I > 2\sigma(I)$
$R_{int} = 0.047$

Refinement

$R[F^2 > 2\sigma(F^2)] = 0.048$
$wR(F^2) = 0.139$
$S = 1.05$
2835 reflections
181 parameters
H-atom parameters constrained
$\Delta\rho_{\max} = 0.28$ e Å^{-3}
$\Delta\rho_{\min} = -0.29$ e Å^{-3}

Compound (II)

Crystal data

$C_{15}H_{15}FN_2O$
$M_r = 258.29$
Monoclinic, $C2/c$
$a = 27.141$ (4) Å
$b = 5.4082$ (7) Å
$c = 17.2849$ (18) Å
$\beta = 103.275$ (9)°
$V = 2469.3$ (6) Å^3
$Z = 8$
Mo $K\alpha$ radiation
$\mu = 0.10$ mm^{-1}
$T = 120$ K
0.41 × 0.27 × 0.10 mm

Data collection

Bruker–Nonius KappaCCD area-detector diffractometer
Absorption correction: multi-scan (*SADABS*; Sheldrick, 2003)
$T_{\min} = 0.961$, $T_{\max} = 0.990$
21463 measured reflections
2824 independent reflections
1511 reflections with $I > 2\sigma(I)$
$R_{\rm int} = 0.092$

Refinement

$R[F^2 > 2\sigma(F^2)] = 0.053$
$wR(F^2) = 0.148$
$S = 1.05$
2824 reflections
173 parameters
H-atom parameters constrained
$\Delta\rho_{\max} = 0.28$ e Å^{-3}
$\Delta\rho_{\min} = -0.23$ e Å^{-3}

Compound (III)

Crystal data

$C_{15}H_{14}FNO_2$
$M_r = 259.27$
Monoclinic, $P2_1/c$
$a = 5.5265$ (5) Å
$b = 10.6652$ (19) Å
$c = 20.905$ (4) Å
$\beta = 97.166$ (11)°
$V = 1222.6$ (3) Å^3
$Z = 4$
Mo $K\alpha$ radiation
$\mu = 0.10$ mm^{-1}
$T = 120$ K
0.26 × 0.25 × 0.14 mm

Data collection

Bruker–Nonius KappaCCD area-detector diffractometer
Absorption correction: multi-scan (*SADABS*; Sheldrick, 2003)
$T_{\min} = 0.974$, $T_{\max} = 0.986$
17136 measured reflections
2807 independent reflections
1657 reflections with $I > 2\sigma(I)$
$R_{\rm int} = 0.061$

Refinement

$R[F^2 > 2\sigma(F^2)] = 0.058$
$wR(F^2) = 0.175$
$S = 1.06$
2807 reflections
173 parameters
H-atom parameters constrained
$\Delta\rho_{\max} = 0.29$ e Å^{-3}
$\Delta\rho_{\min} = -0.40$ e Å^{-3}

Compound (IV)

Crystal data

$C_{15}H_{14}FNOS$
$M_r = 275.34$
Monoclinic, $P2_1/n$
$a = 9.272$ (2) Å
$b = 10.9142$ (13) Å
$c = 12.963$ (2) Å
$\beta = 101.023$ (11)°
$V = 1287.6$ (4) Å^3
$Z = 4$
Mo $K\alpha$ radiation
$\mu = 0.25$ mm^{-1}
$T = 120$ K
0.36 × 0.19 × 0.14 mm

Data collection

Bruker–Nonius KappaCCD area-detector diffractometer
Absorption correction: multi-scan (*SADABS*; Sheldrick, 2003)
$T_{\min} = 0.914$, $T_{\max} = 0.965$
20089 measured reflections
2944 independent reflections
2049 reflections with $I > 2\sigma(I)$
$R_{\rm int} = 0.059$

Refinement

$R[F^2 > 2\sigma(F^2)] = 0.050$
$wR(F^2) = 0.135$
$S = 1.03$
2944 reflections
173 parameters
H-atom parameters constrained
$\Delta\rho_{\max} = 0.65$ e Å^{-3}
$\Delta\rho_{\min} = -0.50$ e Å^{-3}

Compound (V)

Crystal data

$C_{15}H_{14}FNOS$
$M_r = 275.34$
Monoclinic, $P2_1/c$
$a = 9.2106$ (16) Å
$b = 10.906$ (2) Å
$c = 13.4259$ (13) Å
$\beta = 106.086$ (12)°
$V = 1295.8$ (4) Å^3
$Z = 4$
Mo $K\alpha$ radiation
$\mu = 0.25$ mm^{-1}
$T = 120$ K
0.39 × 0.24 × 0.10 mm

Data collection

Bruker–Nonius KappaCCD area-detector diffractometer
Absorption correction: multi-scan (*SADABS*; Sheldrick, 2003)
$T_{\min} = 0.908$, $T_{\max} = 0.975$
20023 measured reflections
2975 independent reflections
1888 reflections with $I > 2\sigma(I)$
$R_{\rm int} = 0.082$

Refinement

$R[F^2 > 2\sigma(F^2)] = 0.048$
$wR(F^2) = 0.106$
$S = 1.03$
2975 reflections
173 parameters
H-atom parameters constrained
$\Delta\rho_{\max} = 0.25$ e Å^{-3}
$\Delta\rho_{\min} = -0.31$ e Å^{-3}

Compound (VI)

Crystal data

$C_{15}H_{14}ClNO_2$
$M_r = 275.72$
Monoclinic, $P2_1/n$
$a = 10.2835$ (13) Å
$b = 5.4829$ (3) Å
$c = 23.428$ (2) Å
$\beta = 96.665$ (9)°
$V = 1312.0$ (2) Å^3
$Z = 4$
Mo $K\alpha$ radiation
$\mu = 0.29$ mm^{-1}
$T = 120$ K
0.42 × 0.18 × 0.14 mm

Data collection

Bruker–Nonius KappaCCD area-detector diffractometer
Absorption correction: multi-scan (*SADABS*; Sheldrick, 2003)
$T_{\min} = 0.889$, $T_{\max} = 0.961$
20222 measured reflections
3017 independent reflections
1902 reflections with $I > 2\sigma(I)$
$R_{\rm int} = 0.073$

Refinement

$R[F^2 > 2\sigma(F^2)] = 0.052$
$wR(F^2) = 0.143$
$S = 1.07$
3017 reflections
173 parameters
H-atom parameters constrained
$\Delta\rho_{\max} = 0.33$ e Å^{-3}
$\Delta\rho_{\min} = -0.44$ e Å^{-3}

Compound (VII)

Crystal data

$C_{16}H_{14}F_3NO_3$
M_r = 325.28
Triclinic, $P\overline{1}$
a = 5.5088 (6) Å
b = 10.7619 (17) Å
c = 13.1398 (19) Å
α = 110.011 (10)°
β = 98.797 (10)°
γ = 92.271 (12)°
V = 719.80 (18) Å^3
Z = 2
Mo $K\alpha$ radiation
μ = 0.13 mm^{-1}
T = 120 K
0.41 × 0.19 × 0.08 mm

Data collection

Bruker–Nonius KappaCCD area-detector diffractometer
Absorption correction: multi-scan (*SADABS*; Sheldrick, 2003)
$T_{\min}$ = 0.949, $T_{\max}$ = 0.990
21281 measured reflections
3299 independent reflections
1690 reflections with $I > 2\sigma(I)$
$R_{\rm int}$ = 0.111

Refinement

$R[F^2 > 2\sigma(F^2)]$ = 0.056
$wR(F^2)$ = 0.147
S = 1.01
3299 reflections
209 parameters
H-atom parameters constrained
$\Delta\rho_{\max}$ = 0.26 e Å^{-3}
$\Delta\rho_{\min}$ = −0.31 e Å^{-3}

Compound (VIII)

Crystal data

$C_{16}H_{14}F_3NO_2S$
M_r = 341.35
Monoclinic, $P2_1/c$
a = 16.234 (3) Å
b = 5.6113 (5) Å
c = 16.665 (3) Å
β = 106.143 (14)°
V = 1458.2 (4) Å^3
Z = 4
Mo $K\alpha$ radiation
μ = 0.26 mm^{-1}
T = 120 K
0.38 × 0.32 × 0.24 mm

Data collection

Bruker–Nonius KappaCCD area-detector diffractometer
Absorption correction: multi-scan (*SADABS*; Sheldrick, 2003)
$T_{\min}$ = 0.906, $T_{\max}$ = 0.939
21849 measured reflections
3348 independent reflections
2493 reflections with $I > 2\sigma(I)$
$R_{\rm int}$ = 0.070

Refinement

$R[F^2 > 2\sigma(F^2)]$ = 0.048
$wR(F^2)$ = 0.128
S = 1.11
3348 reflections
209 parameters
H-atom parameters constrained
$\Delta\rho_{\max}$ = 0.30 e Å^{-3}
$\Delta\rho_{\min}$ = −0.42 e Å^{-3}

Compound (IX)

Crystal data

$C_{15}H_{11}F_3N_2O_5$
M_r = 356.26
Monoclinic, $P2_1/c$
a = 20.4120 (15) Å
b = 7.3690 (18) Å
c = 10.035 (3) Å
β = 103.091 (15)°
V = 1470.2 (6) Å^3
Z = 4
Mo $K\alpha$ radiation
μ = 0.15 mm^{-1}
T = 120 K
0.26 × 0.25 × 0.14 mm

Data collection

Bruker–Nonius KappaCCD area-detector diffractometer
Absorption correction: multi-scan (*SADABS*; Sheldrick, 2003)
$T_{\min}$ = 0.963, $T_{\max}$ = 0.980
18612 measured reflections
2743 independent reflections
1634 reflections with $I > 2\sigma(I)$
$R_{\rm int}$ = 0.081

Refinement

$R[F^2 > 2\sigma(F^2)]$ = 0.062
$wR(F^2)$ = 0.183
S = 1.07
2743 reflections
226 parameters
H-atom parameters constrained
$\Delta\rho_{\max}$ = 0.31 e Å^{-3}
$\Delta\rho_{\min}$ = −0.32 e Å^{-3}

All H atoms were located in difference maps and then treated as riding in geometrically idealized positions, with C—H = 0.95 (aromatic and heteroaromatic), 0.98 (CH_3), 0.99 (CH_2) or 1.00 Å (aliphatic CH), and with $U_{\rm iso}$(H) = $kU_{\rm eq}$(C), where k = 1.5 for the methyl groups, which were permitted to rotate but not to deform or tilt, or 1.2 for all other H atoms. Crystals of (IX) diffracted very weakly at high θ and consquently reflections with $\theta > 25.5°$ were omitted from the final refinements. Despite this, fewer than 60% (1631 out of 2743) of the reflections out to θ = 25.5° were labelled as observed.

For all nine compounds, data collection: *COLLECT* (Nonius, 1999); cell refinement: *DIRAX/LSQ* (Duisenberg *et al.*, 2000); data reduction: *EVALCCD* (Duisenberg *et al.*, 2003); program(s) used to solve structure: *SIR2004* (Burla *et al.*, 2005); program(s) used to refine structure: *SHELXL97* (Sheldrick, 2008); molecular graphics: *PLATON* (Spek, 2009); software used to prepare material for publication: *SHELXL97* and *PLATON*.

The authors thank the Centro de Instrumentación Científico-Técnica of the Universidad de Jaén and the staff for the data collection. AP and MCB thank COLCIENCIAS (grant No. 1102-521-28229) for financial support. JC thanks the Consejería de Innovación, Ciencia y Empresa (Junta de Andalucía, Spain), for financial support.

Supplementary data for this paper are available from the IUCr electronic archives (Reference: SK3430). Services for accessing these data are described at the back of the journal.

References

Acosta, L. M., Bahsas, A., Palma, A., Cobo, J., Low, J. N. & Glidewell, C. (2008). *Acta Cryst.* C**64**, o514–o518.
Bernstein, J., Davis, R. E., Shimoni, L. & Chang, N.-L. (1995). *Angew. Chem. Int. Ed. Engl.* **34**, 1555–1573.
Blanco, M. C., Palma, A., Bahsas, A., Cobo, J. & Glidewell, C. (2009). *Acta Cryst.* C**65**, o487–o491.
Blanco, M. C., Raysth, W., Palma, A., Cobo, J., Low, J. N. & Glidewell, C. (2008). *Acta Cryst.* C**64**, o524–o528.
Brammer, L., Bruton, E. A. & Sherwood, P. (2001). *Cryst. Growth Des.* **1**, 277–290.
Burla, M. C., Caliandro, R., Camalli, M., Carrozzini, B., Cascarano, G. L., De Caro, L., Giacovazzo, C., Polidori, G. & Spagna, R. (2005). *J. Appl. Cryst.* **38**, 381–388.
Cremer, D. & Pople, J. A. (1975). *J. Am. Chem. Soc.* **97**, 1354–1358.
Duisenberg, A. J. M., Hooft, R. W. W., Schreurs, A. M. M. & Kroon, J. (2000). *J. Appl. Cryst.* **33**, 893–898.
Duisenberg, A. J. M., Kroon-Batenburg, L. M. J. & Schreurs, A. M. M. (2003). *J. Appl. Cryst.* **36**, 220–229.
Gómez, S. L., Raysth, W., Palma, A., Cobo, J., Low, J. N. & Glidewell, C. (2008). *Acta Cryst.* C**64**, o519–o523.
Gómez, S. L., Sanabria, C. M., Palma, A., Bahsas, A., Cobo, J. & Glidewell, C. (2009). *Acta Cryst.* C**65**, o465–o469.
Gómez-Ayala, S., Castrillón, J. A., Palma, A., Leal, S. M., Escobar, P. & Bahsas, A. (2010). *Bioorg. Med. Chem.* **18**, 4721–4739.
Howard, J. A. K., Hoy, V. J., O'Hagan, D. & Smith, G. T. (1996). *Tetrahedron*, **52**, 12613–12622.
Nonius (1999). *COLLECT*. Nonius BV, Delft, The Netherlands.
Sheldrick, G. M. (2003). *SADABS*. University of Göttingen, Germany.

Sheldrick, G. M. (2008). *Acta Cryst.* A**64**, 112–122.
Spek, A. L. (2009). *Acta Cryst.* D**65**, 148–155.
Thallypally, P. K. & Nangia, A. (2001). *CrystEngComm*, **3**, 114–119.
Wood, P. A., Allen, F. H. & Pidcock, E. (2009). *CrystEngComm*, **11**, 1563–1571.
Yépez, A. F., Palma, A., Stashenko, E., Bahsas, A. & Amaro-Luis, J. (2006). *Tetrahedron Lett.* **47**, 5825–5828.